Author Manuscript

Author Manuscript

Author Manuscript

Author Manuscript

HHS Public Access

Author manuscript

Nat Chem Biol. Author manuscript; available in PMC 2020 January 01.

Published in final edited form as:

Nat Chem Biol. 2019 January ; 15(1): 88–94. doi:10.1038/s41589-018-0184-3.

N^6-Methyladenosine methyltransferase ZCCHC4 mediates ribosomal RNA methylation

Honghui Ma[#1,2,3], **Xiaoyun Wang**[#4], **Jiabin Cai**[#5], **Qing Dai**[2,3], **S. Kundhavai Natchiar**[6], **Ruitu Lv**[1], **Kai Chen**[2,3], **Zhike Lu**[2,3], **Hao Chen**[1], **Yujiang Geno Shi**[1,7], **Fei Lan**[1], **Jia Fan**[5], **Bruno P. Klaholz**[6], **Tao Pan**[4], **Yang Shi**[1,8], and **Chuan He**[2,3,4]

[1]Liver Cancer Institute, Zhongshan Hospital, Fudan University, and Institute of Biomedical Sciences, Fudan University, Shanghai, China.

[2]Department of Chemistry and Institute for Biophysical Dynamics, The University of Chicago, Chicago, IL, USA.

[3]Howard Hughes Medical Institute, The University of Chicago, Chicago, IL, USA.

[4]Department of Biochemistry and Molecular Biology, The University of Chicago, Chicago, IL, USA.

[5]Liver Cancer Institute, Zhongshan Hospital, Fudan University, Key Laboratory of Carcinogenesis and Cancer Invasion (Fudan University), Ministry of Education, Shanghai, China.

[6]Department of Integrated Structural Biology, Centre for Integrative Biology (CBI), Institute of Genetics and of Molecular and Cellular Biology (IGBMC), CNRS, Inserm, Université de Strasbourg, Illkirch, France.

[7]Endocrinology Division, Brigham and Women's Hospital, Harvard Medical School, Boston, MA, USA.

[8]Department of Cell Biology, Harvard Medical School, Boston, MA, USA.

[#] These authors contributed equally to this work.

Abstract

Correspondence and requests for materials should be addressed to T.P., Y.S. or C.H.

Author contributions

H.M., T.P., Y.S. and C.H. designed the experiments. H.M. purified the recombinant ZCCHC4 protein, established the *ZCCHC4* knockout stable cell lines, and carried out the in vitro and in vivo enzyme activity experiments and rescue experiments. X.W. performed polysome profile sequencing and reporter assays. J.C. performed WB and IHC in liver cancer samples and tumor growth assay in nude mice. Q.D. and K.C. assisted with enzyme activity experiments. R.L. and Z.L. helped with PAR-CLIP analysis. H.C. and Y.G.S. helped measure in vivo enzyme activity. F.L. helped design the experiments. J.F helped prepare patient samples and analyze data. S.K.N. and B.P.K. helped with cryo-EM analysis of the m^{6}A4220 modification site. H.M., X.W, T.P., Y.S. and C.H. wrote the manuscript.

Competing interests

Y.S. is a co-founder of Constellation Pharmaceuticals, Inc., and Athelas Therapeutics. C.H. is a scientific founder of Accent Therapeutics, Inc. and a member of its scientific advisory board.

Additional information

Supplementary information is available for this paper at https://doi.org/10.1038/s41589-018-0184-3.

Reprints and permissions information is available at www.nature.com/reprints.

Publisher's note: Springer Nature remains neutral with regard to jurisdictional claims in published maps and institutional affiliations.

Data availability. All raw data and processed files have been deposited in GSE102336.

Author Manuscript Author Manuscript Author Manuscript Author Manuscript

N^6-Methyladenosine (m^6A) RNA modification is present in messenger RNAs (mRNA), ribosomal RNAs (rRNA), and spliceo-somal RNAs (snRNA) in humans. Although mRNA m^6A modifications have been extensively studied and shown to play critical roles in many cellular processes, the identity of m^6A methyltransferases for rRNAs and the function of rRNA m^6A modifications are unknown. Here we report a new m^6A methyltransferase, ZCCHC4, which primarily methylates human 28S rRNA and also interacts with a subset of mRNAs. *ZCCHC4* knockout eliminates m^6A4220 modification in 28S rRNA, reduces global translation, and inhibits cell proliferation. We also find that ZCCHC4 protein is overexpressed in hepatocellular carcinoma tumors, and *ZCCHC4* knockout significantly reduces tumor size in a xenograft mouse model. Our results highlight the functional significance of an rRNA m^6A modification in translation and in tumor biology.

Reporting Summary.

Further information on research design is available in the Nature Research Reporting Summary linked to this article.

RNA modifications are ubiquitously present in almost all cellular RNAs[1,2]. Methylations are among the most prevalent type of RNA modifications in humans; for example, m^6A is present in tens of thousands of sites in mRNA and long noncoding RNA, as well as in 18 S and 28S rRNA and U2, U4 and U6 spliceosomal RNA[1,3,4]. Distributions of m^6A modification on mRNAs revealed by high-throughput sequencing strongly suggest that m^6A impacts a wide range of physiological and pathological processes, such as stem cell pluripotency[5,6], microRNA biogenesis[7], RNA structural switches[8], stress responses[9,10], and cancer[11,12]. Although mRNA m^6A modifications have been extensively studied and have been shown to play critical roles in numerous biological systems, the identity of m^6A methyltransferases for rRNAs and function of rRNA m^6A modifications are unknown.

Human rRNA contains chemical modifications at approximately 210 sites, most of which are 2′O-methylations (Nm) and pseudouridines (Ψ)[13]. 2′OMe and Ψ modifications in rRNA are typically installed by small-nucleolar RNA (snoRNA) guides together with catalytic and regulatory protein subunits that form snoRNPs[14]. Two m^6A modifications are known to be present in rRNA, one in 28S rRNA at position 4220 and the other in 18 S rRNA at position 1832 (refs. [13,15,16]). Human rRNA modifications are introduced during ribosome biogenesis; rRNA modifications in the mature ribosome have been implicated in regulation and activity tuning of protein synthesis because they tend to localize in functionally important regions[17]. The effects of rRNA modifications on translation regulation could have potential implications for human health; therefore, identification of new enzymes responsible for rRNA modifications could be important not only for revealing additional mechanisms for translation regulation but also for designing selective inhibitors and potential therapeutic agents. Though RNA m^6A methyltransferases METTL3-METTL14 and METTL16 are known for mediating m^6A methylation on mRNA and noncoding RNAs[1,18–26], identities of m^6A methyltransferases for human rRNAs remain unknown. Methylation of nucleotides in rRNAs is a ubiquitous feature that occurs in all living organisms[16]. Most functional studies on eukaryotic rRNA modifications have been performed in yeast; however, yeast rRNAs do not contain these m^6A modifications[13].

Author Manuscript Author Manuscript Author Manuscript Author Manuscript

A previous bioinformatics study suggested the CCHC zinc-finger-containing protein ZCCHC4 (UniProt accession number Q9H5U6) as a potential RNA methyltransferase[27]. CCHC zinc-finger-containing proteins are the most common zinc finger proteins in eukaryotes and are well known for their functions in regulating various RNA-dependent biological processes[28]. The CCHC-ZnF domain is one of the canonical nucleic acid-recognition domains in both DNA-and RNA-binding proteins; binding of CCHC zinc-finger-containing protein to target RNAs can regulate gene expression and translation[28,29]. For example, ZC3H13, a zinc-finger protein, has been reported to regulate nuclear RNA m^{6}A methylation and mouse embryonic stem cell self-renewal[30]. We found that the *ZCCHC4* gene is conserved in other multicellular model organisms but absent in yeast (Supplementary Fig. 1a). Upon further analysis of functional domains of ZCCHC4 protein (Fig. 1a), we noticed that ZCCHC4 possesses a potential N^6-methyladenosine methyltransferase domain with a conserved catalytic motif, 'DPPF', and a CCHC-ZnF domain.

Here, we show that ZCCHC4 is an RNA m^{6}A methyltransferase that methylates human 28S rRNA in vitro and in vivo. Furthermore, we show that the ZCCHC4-mediated rRNA m^{6}A methylation impacts ribosome subunit distribution, global translation and cell proliferation. We also show that ZCCHC4 protein is aberrantly expressed in tumor tissues, and its deletion has a large impact on tumor growth in a mouse model. These results reveal the importance and the critical function of a single base methylation in human rRNA.

Results

ZCCHC4 is an m^{6}A RNA methyltransferase.

To determine whether ZCCHC4 has methylation activity in vitro, we cloned, expressed and purified full-length recombinant ZCCHC4 protein (Supplementary Fig. 1b) and performed in vitro enzymatic assays using wild-type (ZCCHC4 WT) protein and a predicted, catalytically inactive mutant (ZCCHC4 4 A) after changing key residues (276–279) "DPPF" to "AAAA" (Fig. 1a). We incubated the recombinant protein with three different RNA probes bearing distinct substrate motifs (GGACU, GAACU and AAACU), in accordance with the consensus sequence of ([G/A][G > A]m^{6}AC[U > A > C]) found in mammalian mRNA m^{6}A methylation. We monitored reactions using liquid chromatography-tandem mass spectrometry (LC-MS/ MS). We found that ZCCHC4 specifically installed a methyl group on an AAC-motif-containing probe but exhibited no observable activity toward a GAC-motif-containing probe, with the probe bearing the GAACU motif serving as a better substrate than the AAACU-containing probe (Fig. 1b). Previous studies reported that the mRNA m^{6}A methyltransferase complex METTL3-METTL14 displayed higher activity toward a GAC-containing motif than the AAC-containing probe[21], suggesting that ZCCHC4 may preferentially mediate m^{6}A methylation of RNAs with an AAC motif. Interestingly, both mammalian 18 S and 28S rRNAs have one m^{6}A site embedded in an AAC but not a GAC motif, raising the possibility that ZCCHC4 may methylate rRNA.

ZCCHC4 methylates 28S rRNA in vitro.

Our western blotting analysis showed that ZCCHC4 was present in both the cytoplasm and the nucleus (Supplementary Fig. 1c), which was confirmed using immunofluorescence

Author Manuscript Author Manuscript Author Manuscript Author Manuscript

assays. ZCCHC4 was further shown to accumulate in the nucleolus (Supplementary Fig. 1c,d), where ribosome biogenesis takes place[31], which is consistent with our hypothesis that ZCCHC4 may function to methylate rRNA. To address this possibility, we synthesized two 12-mer RNA probes representing m^6A-bearing 18 S and 28S rRNA, respectively. After incubating these probes with purified ZCCHC4 protein and co-factor d_3-SAM, a new peak representing 28S rRNA probe with an added methyl group was detected by MALDI mass spectrometry. This new peak was not observed when catalytically inactive ZCCHC4 was used (Fig. 1c). A significantly weaker activity was detected when the 18 S rRNA probe was tested (Supplementary Fig. 1e). Reaction product was further digested and quantified by LC-MS/MS, and results showed that enzyme activity of ZCCHC4 for 28S rRNA probe was about 24-fold higher than that for the 18 S rRNA probe (Fig. 1d). These results suggest that ZCCHC4 could be a human RNA m^6A methyltransferase for the 28S rRNA.

ZCCHC4 catalyzes 28S rRNA methylation in cells.

To identify RNA substrates of ZCCHC4 in vivo, we employed photoactivatable ribonucleoside-enhanced cross-linking and immunoprecipitation (PAR-CLIP)[32,33]. ZCCHC4-bound RNAs were extracted for RNA sequencing to identify RNA substrates of ZCCHC4 in cells (Supplementary Fig. 2a-d, Supplementary Dataset 1). Results showed that main binding targets of ZCCHC4 were 28S rRNAs (Fig. 2a), and the region containing the highest sequencing coverage among ZCCHC4 PAR-CLIP peaks on 28S rRNA were residues 1854–1913 (Fig. 2b). In the three-dimensional structure of the 60 S large ribosomal subunit (PDB ID 6EK0), residues 1854–1913 are proximal to the m^6A 4220 residue (Supplementary Fig. 3a), and all ZCCHC4-bound regions in 28S rRNA are in close special proximity to the m^6A 4220 site (Supplementary Figs. 3b,c), supporting the notion that ZCCHC4 binds and methylates this site.

To verify the methylation activity of ZCCHC4 on 28S rRNA, we knocked out *ZCCHC4* in both HepG2 and HeLa cells using CRISPR-Cas9. There are two isoforms of *ZCCHC4* in humans, a long one with all exons and a short one containing the methyltransferase domain (Supplementary Fig. 4a). We designed different sgRNAs targeting exon 1, which only affected the long isoform (designated as KO1), exon 4, which affected both isoforms (designated as KO4), or exon 7, which deleted the methyltransferase domain (designated as KO7). We pulled down 28S rRNA from different KO and WT cells using a specific 40-nucleotide (nt) biotin-labeled DNA oligo complementary to the methylation region containing the A4220 site. RNA fragments were digested to mononucleotides, and the amount of m^6A was quantified by LC- MS/MS (Supplementary Fig. 4b). Compared to WT cells, cells with sgRNA targeting exon 1 still had 20% m^6A (Fig. 2c), suggesting that the short isoform also contributed to residual m^6A methylation. In contrast, m^6A was almost lost in cells with sgRNA targeting exon 4 or exon 7 (Fig. 2c). We obtained essentially the same results with *ZCCHC4* knockout in HeLa cells (Supplementary Fig. 4c). We also incubated total RNAs from WT and KO cells with recombinant ZCCHC4 protein and cofactor *d*3-SAM in vitro, which was followed by pull down of 28S rRNA m^6A4220-containing fragment, digestion to single nucleosides and LC-MS/MS analysis to measure d_3m^6A level. Our results showed that recombinant ZCCHC4 protein also installed m^6A on 28S rRNA in vitro (Supplementary Fig. 4d).

Author Manuscript Author Manuscript Author Manuscript Author Manuscript

To determine whether loss of m^6A in the 28S rRNA was indeed due to loss of ZCCHC4, we carried out genetic rescue experiments (Fig. 2d). Individual RNA species (28S rRNA, 18 S rRNA and mRNA) from HepG2 cells were extracted to measure m^6A levels by LC-MS/ MS. The m^6A modification on 28S rRNA almost completely disappeared upon *ZCCHC4* knockout, whereas 18 S rRNAs or mRNAs showed no noticeable changes in the KO cells (Fig. 2e). Importantly, loss of m^6A in 28S rRNA was completely recovered by expressing ZCCHC4 WT, but not enzymatically dead mutant ZCCHC4 (DPPF changed to AAAA) protein, or by transfecting control vector (Fig. 2e). The same rescue experiments were repeated in HeLa cells with similar results obtained (Supplementary Fig. 5a,b).

To confirm the precise methylation site and determine methylation fraction, we isolated the 28S rRNA fragment using biotin labeled 40-nt DNA oligo complementary to the rRNA A4220 region. We then digested the pull-down product with RNases A and T1 and carried out HPLC analysis. Using AACp or A(m^6A)Cp as standards, we found that ~55% AAC was methylated at the A4220 site in wild-type cells. Although the A(m^6A)C peak completely disappeared in *ZCCHC4* KO cells, this peak could be rescued by transfection of ZCCHC4 WT plasmid, but not the catalytically dead mutant plasmid (Supplementary Fig. 5c). Together, these results indicate that ZCCHC4 is the main methyltransferase responsible for the m^6A4220 methylation in human 28S rRNA.

ZCCHC4 affects translation in cells.

Modifications on rRNA affect many aspects of ribosome structure, assembly, and dynamics[34,35]. We investigated whether ZCCHC4-mediated rRNA methylation associates with mature rRNA levels. Total RNAs extracted from WT and *ZCCHC4* KO cells were subjected to denaturing gel (Supplementary Fig. 6a,b) and qRT-PCR analysis (Supplementary Fig. 6c) to compare 18 S and 28S rRNA levels in Wt and kO cells. Our results showed that *ZCCHC4* knockout did not noticeably change the levels of mature rRNAs. Considering that ~55% of the A4220 residue in 28S rRNA was methylated by ZCCHC4 (Supplementary Fig. 5c), ZCCHC4 may not substantially affect prerRNA processing.

We next analyzed the localization and environment of m^6A4220 modification in the high-resolution cryo-EM structure of human 80 S ribosome (PDB 6EK0)[17,36]. The m^6A4220 modification site is only partially buried and is close to the surface of 60 S ribosomal subunit; it is oriented toward 40 S subunit side approaching the ribosomal subunit interface (Supplementary Fig. 7a,b). The N^6-methyl group extends the plane of the A4220 base and increases the stacking interaction with the two neighboring bases of G4222 and A4219. These three bases are offset in such a way that a gap would be present in their stacking without the m^6A modification (Supplementary Fig. 7a-f). This structural analysis suggests that ZCCHC4-mediated rRNA methylation likely affects ribosome structure and subunit assembly. To examine the effect of m^6A4220 depletion on ribosomal subunit distribution in cells, we carried out sucrose density gradient (SDG) at low Mg^{2+} concentration according to an established protocol[35]. We found that the ratio of the 60 S ribosomal subunit peak over the 80 S peak markedly decreased in *ZCCHC4* KO cells compared to WT cells. Importantly, the 60 S subunit peak in *ZCCHC4* KO cells was rescued by WT plasmid but not by

Author Manuscript Author Manuscript Author Manuscript Author Manuscript

catalytically dead mutant plasmid. These results (Fig. 2f) suggest that ZCCHC4 plays a role in controlling ribosome subunit levels.

We next investigated whether ZCCHC4 impacts protein translation. We measured the difference in translational activities between WT and *ZCCHC4* KO cells in two ways. First, we used a luciferase reporter, which showed that WT cells produced higher luciferase levels than KO cells (Fig. 3a). We also measured global protein synthesis activity using L-homopropargylglycine derived metabolic labeling of newly synthesized proteins (Fig. 3b). We found that KO cells displayed ~25% reduction in global translation compared to WT cells (Fig. 3b), and global translation activity in *ZCCHC4* KO cells can be restored by transfection of WT flag-ZCCHC4 plasmid but not catalytically dead mutant flag-ZCCHC4 plasmid (Fig. 3c). These results support our hypothesis that ZCCHC4 affects global translation, most likely through its 28S rRNA m^6A methylation activity.

To further investigate the effect of ZCCHC4 on translation, we performed polysome profiling of WT and *ZCCHC4* KO cells by SDG and by polysome-associated mRNA sequencing. SDG profiles showed that the amount of polysomes compared to the 80 S monosome peak was significantly reduced in *ZCCHC4* KO cells relative to the wild-type cells (Fig. 3d). Polysome-associated mRNA sequencing showed that for all genes, KO cells showed a broader profile for mRNA(polysome)/mRNA(input) ratios, suggesting that loss of the 28S rRNA m^6A modification reduced the tight control of translation on mRNA populations (Fig. 3e; Supplementary Dataset 2). ZCCHC4-bound mRNAs (PAR-CLIP targets) showed a biased shift in KO cells, suggesting that loss of ZCCHC4 might increase translation for a subset of its mRNA interacting partners (Fig. 3f; Supplementary Dataset 2). Gene ontology analysis of ZCCHC4-bound mRNAs with $\log_2(WT/KO) > 0.5$ and < -0.5 (311 genes in total) showed that genes affected by ZCCHC4 were involved in membrane protein targeting, mRNA catabolic process, ER localization, and translation initiation (Supplementary Fig. 8; Supplementary Dataset 2). Gene ontology analysis further suggested that ZCCHC4 might play additional roles to affect translation through its binding to a subset of mRNAs (Supplementary Fig. 8; Supplementary Dataset 2), which requires further investigation in the future.

ZCCHC4 expression affects cancer progression.

We next investigated whether ZCCHC4-mediated rRNA methylation affects cell proliferation. We found that cell proliferation was markedly reduced in three independently constructed *ZCCHC4* knockout HepG2 cell lines compared to WT controls (Supplementary Fig. 9a). Importantly, decreased proliferation of KO cells was partially rescued by transfecting wild-type ZCCHC4 plasmid, but not cat-alytically dead mutant plasmid or empty-vector control (Fig. 4a). These results are consistent with our observed effects of ZCCHC4 on translation.

To further address the role of ZCCHC4 in cell proliferation, we investigated potential roles of ZCCHC4 in cancer. We measured the expression level of the ZCCHC4 protein in hepatocellular carcinoma tumor (HCT) tissues compared to immediately adjacent normal tissues (para tissues). We found that many HCT tumors exhibit overexpression of the ZCCHC4 protein compared to corresponding para tissues (Fig. 4b). We collected cancer

Author Manuscript Author Manuscript Author Manuscript Author Manuscript

tissues and para tissues from a total of 180 patients and measured ZCCHC4 expression using immunohistochemistry (IHC). Among 180 tumor tissues examined, 93 (52%) had higher, 81 (45%) comparable, and only 6 (3%) decreased ZCCHC4 levels than the corresponding para tissues of the same patient (Fig. 4c). We also extracted 28S rRNA from tumor and para tissues of six patients and analyzed their m^6A levels by LC-MS/MS. Consistently, m^6A levels in 28S rRNA from tumor tissues are higher than para tissues in five of these six patients (Supplementary Fig. 9b). Lastly, we examined the relationship between ZCCHC4-mediated m^6A methylation and tumor progression. HepG2 wild-type, KO1# 1, and KO1# 2 cells (~5×10^6 each) were used in a mouse subcutaneous (SC) xenograft tumor model. *ZCCHC4* KO cells showed notable reduction of tumor growth measured by volume or by weight in nude mouse models compared to WT cells (Fig. 4d; Supplementary Fig. 9c). These results support the role of the ZCCHC4-catalyzed rRNA methylation in cancer cell growth and tumor progression.

Discussion

In this work we report the discovery of a human rRNA m^6A methyl-transferase, ZCCHC4. This is the first m^6A methyltransferase found to mediate m^6A methylation of eukaryotic, cytosolic rRNAs. Several m^6A modifications have been identified in bacterial rRNAs[35,37,38]. *Escherichia coli* 23 S rRNA contains two m^6A sites in the central region of the 50 S ribosomal subunit[37]. It has been shown that E. coli 23 S rRNA m^6A modifications facilitate stacking interactions with other bases and act as molecular glues to keep distant parts of rRNA together. These bacterial m^6A modifications stabilize the tertiary structure of the ribosome and exert translational control of proteins involved in iron homeostasis and anaerobic growth[38]. Our results show that ZCCHC4-catalyzed m^6A4220 methylation in 28S rRNA is required for optimal global translation activity, which affects cell proliferation and impacts tumor growth. Thus, a single base methylation could have a profound impact on cell physiology.

m^6A modification has not been studied previously in eukaryotic rRNAs, perhaps due to its absence in *Saccharomyces cerevisiae,* in which most rRNA modification studies have taken place so far. We have found that the *ZCCHC4* gene is conserved in multicellular organisms, but absent in single cell eukaryotes, consistent with yeast lacking this particular m^6A modification. Conservation of the *ZCCHC4* gene in multicellular organisms suggests that m^6A is also present in their 28S rRNAs. The reason for the absence of this m^6A modification in yeast is unclear, but the defects of human ribosomes caused by the lack of this modification are most likely compensated by other factors in yeast ribosomes.

A hallmark of mRNA m^6A modification is its cell type and cell state dependent pattern, which requires the actions of the METTL3-METTL14 writer complex and FTO and ALKBH5 eraser proteins[1,18,39–43]. Recently, ALKBH1 has been identified as a tRNA m^1A demethylase, which helps alter m^1A modification fractions in specific tRNAs[44,45]. An intriguing question is whether any rRNA modification is also reversible and thus subjected to dynamic regulation by erasers in cells. Although most of rRNA modifications are buried in mature ribosome, modifications at the 60 S and 40 S interface are occasionally accessible. Furthermore, damaged ribosomes in cells may require disassembly by removing some of the

Author Manuscript Author Manuscript Author Manuscript Author Manuscript

rRNA modifications for complete degradation. Further studies are needed to reveal whether rRNA modifications may also be subject to dynamic reversal by cellular enzymes.

In summary, we discovered a new human RNA m^6A methyltransferase ZCCHC4, which mediates methylation of A4220 on 28S rRNA within an AAC motif. rRNA methylation by ZCCHC4 appears to play a role in cell proliferation regulation and possibly in tumorigenesis. Further studies will reveal (i) the structural defect of ribosomes lacking this methylation, and (ii) the selectivity of methylated ribosome in translational regulation of specific mRNAs and the mechanism of this modification in regulating tumorigenesis.

Online content

Any methods, additional references, Nature Research reporting summaries, source data, statements of data availability and associated accession codes are available at https://doi.org/10.1038/s41589-018-0184-3.

Methods

Plasmid construction and protein expression of recombinant ZCCHC4.

Flag-HA-tagged ZCCHC4 wild-type and mutation plasmids were constructed with pPB-CAG vector using BglII and XhoI sites for expression in mammalian cells. Recombinant ZCCHC4 wild-type and mutation plasmids were cloned into modified pGEX-6p-1, and then transformed into *E. coli* BL21(DE3). Catalytically inactive 4A-mutant plasmids were constructed using QuickChange Site-Directed Mutagenesis Kit.

To express recombinant ZCCHC4, cells were incubated at 37 °C until OD_{600} reached ~ 0.6–1 and then cooled down to 16 °C. IPTG was added to 0.2 mM final concentration, and cells were further incubated at 16 °C for 16 h. Cell pellets were lysated in a buffer containing 300 mM NaCl, 25 mM Tris pH 7.5, DNase (1:1,000), RNase A (1:1,000). Total lysate was passed through GST beads twice, and bound proteins were washed with 200 ml lysis buffer. GST tag was removed by cutting with “3 C” proteases overnight, and ZCCHC4 protein was eluted with elution buffer (20 mM Tris pH7.5, 150 mM NaCl) in 1 ml aliquots until color change was no longer observed according to a Bradford assay. Proteins isolated from GST beads were further purified with mono-S column, washed with buffer A (20 mM Tris pH7.5) and eluted with buffer B (20 mM Tris 7.5, 1 M NaCl).

Isolation of a defined rRNA fragment for QQQ and HPLC analysis.

To isolate the region of 28S rRNA that contains A4220, 2,000 pmol of a synthetic oligo deoxynucleotide (5’ biotin-CTCGCCTTAGGACACCTGCGTTACCGTTTGACA GGTGTAC), complementary to the C4200-C4240 nucleotide region of 28S rRNA, were incubated with 200 pmol of total RNA, in 0.3 volumes of hybridization buffer (250 mM HEPES pH 7, 500 mM KCl). The hybridization mixture was incubated at 90 °C for 7 min and slowly cooled to room temperature (25 °C) over 3.5 h to allow hybridization to occur. Single-stranded RNA and DNA were digested with mung bean nuclease (New England BioLabs) and RNase A over 1 h at 37 °C in a buffer solution (50 mM NaOAc pH 5, 30 mM NaCl, and 1 mM ZnCl2). Digestion products were mixed with streptavidin T1 beads in IP

Author Manuscript Author Manuscript Author Manuscript Author Manuscript

buffer (150 mM NaCl, 50 mM Tris, pH7.9, 0.1% NP40) at 4 °C for 1 h. After washing, beads were heated at 70 °C for 5 min and supernatant (containing 40 nt RNA fragment) was collected.

HPLC analysis AAC and A(m^{6}A)C from 40-nt RNA fragment.

Synthesized AACp or A(m^{6}A)Cp were used as standard, two 16-mer RNA oligos (DP-559–9- 16mer:5'-UCAAACGGUA**A**CGCAG,DP-559–10-16mer:5'-UCAAACGGUA **m^{6}A**CGCAG), whose sequences are part of the 40-mer sequence: GUACACC UGUCAAACGGUA(A/m^{6}A)CGCAGGUGUCCUAAGGCGAG. 40-nt RNA fragments from samples were digested with RNase A and RNase T1 (which cuts after G, U C but not A) and analyzed through HPLC[46].

Construction of *ZCCHC4* KO cell lines using CRISPR.

ZCCHC4 KO cells were generated using a CRISPR-Cas9 approach[47]. To knock out exon 1, sgRNA GTGCCGGGGAAGCTCGGGAA was cloned into pX335; all other knock outs were cloned into pX459: for exon 4, sgRNA GGGGCAACATAGTGAGCATC; for exon 7, sgRNA AGTATGCAGAGCATTTTTACA and sgRNA TGGAAAGAAGGTCAAAGCCA. 1 μg sgRNA was transfected into HepG2 cells with Lipofectamine 2000, and each clone was picked out by diluting cells into 96-well plates. After 3 weeks, the genome of target region from each clone was amplified by PCR and sequenced. Protein levels from knock out clone were checked by western blot with ZCCHC4 antibody.

Rescue experiments with empty vector, flag-ZCCHC4 wild-type, and flag- ZCCHC4 inactive mutant plasmids.

Flag-ZCCHC4 wild-type and flag-ZCCHC4 mutation were cloned into plenti-6.2 vector. Plenti-6.2 empty vector and flag-ZCCH4 WT and mutated plasmids were packaged as lentivirus in 293 T cells. Wild-type HepG2 and HeLa were infected with virus generated by empty vector as a control, whereas knockout cells were infected with virus generated by empty vector, wild-type and mutated ZCCHC4, respectively. After selection with 5 μg/ml blasticidin, cells were collected for rescue experiments.

mRNA isolation.

Total RNA was extracted from wild-type or knockout cells with TRIzol reagent (Invitrogen). mRNA was purified using Dynabeads mRNA DIRECT kit (Ambion), which was followed by further removal of contaminated rRNA using RiboMinus Eukaryote Kit v2 (Ambion). Concentration of mRNA was measured by Qubit RNA HS Assay Kit with Qubit 2.0.

Assays for m^{6}A methyltransferase activity in vitro.

In vitro methyltransferase activity assay was performed in a 30 μL of reaction mixture containing the following components: 4 μg RNA probes, 4 μg fresh recombinant protein (ZCCHC4 WT or ZCCHC4 4 A mutant), 0.8 mM d3-SAM, 50 mM Tris-HCl, 5 mM MgCl2, 1 mM DTT, pH 8.0. The reaction was incubated at 16 °C overnight. After incubation, samples were treated with proteinase K at 50 °C for 20 min, and resultant RNA was desalted and then digested with nuclease P1 and alkaline phosphatase. Nucleosides were quantified

Author Manuscript Author Manuscript Author Manuscript Author Manuscript

by using nucleoside-to-base ion mass transitions of 285 to 153 (*d3*-m^6A) and 284 to 152 (guanosine). Guanosine (G) served as an internal control to calculate the amount of RNA probe in each reaction mixture for QQQ LC-MS/MS analysis. rRNA probe sequences are 28S, 5'-CGGUAACGCAGG-biotin; 18 S, 5'-UCGUAACAAGGU-biotin. Methylation reactions with rRNA probes were performed using described protocol, and desalted resultant RNA was directly analyzed by MALDI mass spectrometry.

LC-MS/MS.

100 ng of mRNA or rRNA (28S, 18 S), isolated from agarose gel, were digested by nuclease P1 (1 U, Wako) in 25 μl of buffer containing 25 mM NaCl and 2.5 mM of $ZnCl_2$ at 42 °C for 2 h, which was followed by addition of NH_4HCO_3 (1 M, 3 μl, freshly made) and alkaline phosphatase (1 U, sigma) and additional incubation at 37 °C for 2 h. Samples were then diluted to 60 μl and filtered (0.22 μm pore size, 4 mm diameter, Millipore); 5 μl of solution was loaded into LC-MS/MS (Agilent6410 QQQ triple-quadrupole mass spectrometer). Nucleosides were quantified by using retention time and nucleoside to base ion mass transitions of 284 to 152 (G), 282.1 to 150.1 (m^6A), and 268 to 136 (A).

PAR-CLIP and RNA sequencing.

PAR-CLIP was followed according previously reported procedures[32,33,48]. HeLa cell lines stably expressing flag-tagged ZCCHC4 were used for PAR-CLIP experiments. Briefly, 4SU (4-thiouridine) was added to cell culture medium at a final concentration of 100 μM. After 14 h of incubation, cells were irradiated, on ice, using Stratalinker 2400 (Stratagene) at 365 nm twice at 0.15 J/cm^2. Flag-ZCCHC4 was immunoprecipitated with anti-flag M2 magnetic beads. We performed RNase T1 digestion, using 0.2 U/μL, for 15 min, for the initial cleavage in lysates, and 50 U/μL, for 15 min, for the second digestion on beads. ^{32}P-labeled RNAs were extracted from SDS-PAGE gel, and RNA libraries were prepared using NEBNext Small RNA Library kit (E7330S). Qualified RNA libraries were sequenced using Illumina HiSeq 2000 with single-end 100-bp read length. Each experiment was conducted with two biological replicates.

Polysome profiling.

Polysome profiling was adapted from previously reported procedures[32,33,49]. Three 15-cm plates of HepG2 cells were prepared for each sample (wild-type and *ZCCHC4* KO). Cells were treated with cycloheximide (CHX), at 100 μg ml^{-1} for 10 min before collection. Cells were lysed on ice for 30 min in 1 ml lysis buffer (10 mM Tris-HCl pH7.4, 5 mM $MgCl_2$, 100 mM KCl, 1% Triton X-100, 2 mM DTT, 500 U/ml RNase inhibitor, 100 μg/ml CHX, protease inhibitor cocktail). Supernatant (~1 ml) was collected, and absorbance at 260 nm (A_{260}) was measured. Samples with equal A_{260} were loaded onto a 10–50% (w/v) sucrose gradient buffer (20 mM HEPES, pH 7.4, 100 mM KCl, 5 mM $MgCl_2$, 2 mM DTT, 100 μg/ml cycloheximide, 1× protease inhibitor cocktail (EDTA-free), 20 U/ml SUPERase inhibitor) prepared using gradient station (Biocomp). 10% of cell lysate for each sample was used as an input (RNA was extracted with Trizol). Gradients were centrifuged at 4 °C for 4 h at 28,000 r.p.m. (Beckman, rotor SW28). Samples were then fractioned and analyzed by Gradient Station (Biocomp) equipped with an ECONO UV monitor (Bio-Rad) and fraction

Author Manuscript Author Manuscript Author Manuscript Author Manuscript

collector (FC203B, Gilson). Fractions corresponding to polysomes from the sucrose gradient were pooled to isolate total RNA by TRIzol reagent.

Extracted RNAs from input and polysome fraction were used to generate the library using TruSeq stranded mRNA sample preparation kit (Illumina). Qualified RNA libraries were sequenced using Illumina HiSeq 2000 with paired-end 100-bp read length. Each experiment was conducted with three biological replicates.

Cell growth analysis and luciferase assay.

1×10^5 cells were seeded in one well of a six-well plate and counted from day 2. Cell number was measured every 2 d with Countess automated cell counter (Life Technologies) following standard procedures and default parameter settings. For luciferase assay, 3×10^4 cells were seeded in a 96-well plate with eight replicates. 1,000 ng of pmirGLO plasmid were transfected into cells using FuGENE HD Transfection Reagent, and cells were incubated at 37 °C in a CO_2 incubator for 48 h. Luciferase activity was measured using Dual-Glo Luciferase Reagent (Promega Corporation) to obtain firefly and renilla luminescence separately. Ratio of firefly/renilla luminescence was calculated for WT and KO cells ($n = 8$, biologically independent samples).

Patients, tissue microarrays (TMAs) and immunohistochemistry.

One specimen cohort ($n = 180$) was randomly collected from consecutive patients with HCC who underwent curative resection, from 2007 to 2008, at the Liver Cancer Institute of Fudan University (Shanghai, China). Histopathological diagnoses were based on World Health Organization criteria. Ethical approval was obtained from the research ethics committee of Zhongshan Hospital, and written informed consent was obtained from each patient. Immunohistochemistry was performed using a two-step protocol. Briefly, sections were dewaxed, hydrated, and washed. After neutralization of endogenous peroxidase (0.3% H_2O_2 for 20 min) and antigen retrieval, slides were preincubated with blocking serum and then incubated at 4 °C overnight with primary antibody. Subsequently, sections were serially rinsed, incubated with secondary antibody, and treated with horseradish peroxidase-conjugated streptavidin. Reaction products were visualized using 3,30-diaminobenzidine tetrahydrochloride and counterstained with hematoxylin. ZCCHC4 antibody was ordered from Abcam: ab209901, secondary antibody was ordered from MXB Biotechnologies: KIT-5010.

In vivo tumor growth assay.

Male, athymic BALB/c nude mice (6-week old) were purchased from Shanghai Institute of Material Medicine of Chinese Academy of Science in Shanghai, and mice were raised under specific pathogen-free conditions.

HepG2 wild-type, KO1# 1 and KO1# 2 cells (about 5×10^6) were used to establish subcutaneous (SC) xenograft tumor models. Tumor size was monitored weekly. Mice were sacrificed after 4 weeks, and tumor weight and two dimensions of tumors were measured.

Author Manuscript Author Manuscript Author Manuscript Author Manuscript

Sequencing data analysis.

For PAR-CLIP, adapters were trimmed by using FASTX-Toolkit. Sequencing data was aligned to the reference human genome version GRCh38/hg38, allowing for, at most, two mismatches. PAR-CLIP data were analyzed by PARalyzerv1.1 with default settings. Binding motif was analyzed by HOMER (v4.7), and the T-to-C mutation was used for identification of 4SU-PAR- CLIP binding sites. Enrichment fold was calculated as log2(IP/input). mRNA-seq and polysome profiling were analyzed by DESeq to generate RPKM (reads per kilobase, per million reads).

Measurement of protein synthesis rate.

Protein synthesis rate was measured by using Click-iT HPG Alexa FluorTM 488 Protein Synthesis Assay Kit (Thermo Fisher: C10428). Briefly, HPG (50 μM final concentration) was added to culture medium and incubated for 30 min, cells were collected by trypsin digestion and fixed with 3.7% formaldehyde in PBS for 15 min, followed by a permeabilization step using 0.5% Triton X-100 for 20 min. The azide-alkyne reaction was performed with the Click-iT reaction cocktail for 30 min at room temperature. Cells were washed with rinse buffer and resuspended in PBS buffer. For flow cytometric analysis, all sorted fractions were double sorted to ensure high purity. Data was analyzed by FlowJo software (Tree Star).

Ethics statement.

The animal care and experimental protocols were carried out in accordance with procedures and guidelines established by Shanghai Medical Experimental Animal Care Commission, all animal experiments were approved by Fudan University Institutional Committee.

Statistics and reproducibility.

For in vitro enzyme activity, data for Fig. 1b-d and Supplementary Fig. 4d are from $n = 2$ independent experiments. For LC-MS/ MS detected m^6A/A level, data for Fig. 2c,e, Supplementary Figs. 4c and 5b are from $n = 3$ independent experiments. Raw data of western blots are provided in Supplementary Fig. 10. P values were determined using two-tailed Student's unpaired t-test for cell proliferation (Fig. 4a; Supplementary Fig. 9a), reporter assay (Fig. 3a), and protein synthesis (Fig. 3b,c). Error bars represent mean ± s.d., $^{*}P < 0.05$, $^{**}P < 0.01$, n.s., not significant. For tumor growth (Fig. 4d), bottom left, error bars represent mean ± s.d., two-way ANOVA was used for comparisons between groups, $^{***}P < 0.001$; bottom right, the values are expressed with Box and Whisker Plot. Plot: Min to Max. Student t-test and one-way analysis of variance were used for comparisons between groups. $^{***}P < 0.001$.

Supplementary Material

Refer to Web version on PubMed Central for supplementary material.

Acknowledgements

We thank X. Wang, L. Hu, H. Shi, F. Liu, and J. Wei from C.H's laboratory for discussions and for sharing experiments materials. We thank J. Tauler for editing the manuscript. This work was supported by the National

Author Manuscript Author Manuscript Author Manuscript Author Manuscript

Institutes of Health grants HG008935 (to C.H.) and GM113194 (to T.P. and C.H.). C.H. is an investigator of the Howard Hughes Medical Institute (HHMI). This work also supported by National Natural Science Foundation of China (81602513; to J.C.) and funds from Fudan University, H.M. is supported by the Postdoctoral International Exchange Program of the China Postdoctoral Council (CPC). X.W. is supported by the National Institute of Diabetes and Digestive and Kidney Diseases of the National Institutes of Health under Award Number 1K01 DK111764.

References

1. Roundtree IA, Evans ME, Pan T & He C Dynamic RNA modifications in gene expression regulation. Cell 169, 1187–1200 (2017). [PubMed: 28622506]
2. Fu Y, Dominissini D, Rechavi G & He C Gene expression regulation mediated through reversible m^6A RNA methylation. Nat. Rev. Genet. 15, 293–306 (2014). [PubMed: 24662220]
3. Gilbert WV, Bell TA & Schaening C Messenger RNA modifications: form, distribution, and function. Science 352, 1408–1412 (2016). [PubMed: 27313037]
4. Zhao BS, Roundtree IA & He C Post-transcriptional gene regulation by mRNA modifications. Nat. Rev. Mol. Cell Biol. 18, 31–42 (2017). [PubMed: 27808276]
5. Batista PJ et al. m^6A RNA modification controls cell fate transition in mammalian embryonic stem cells. Cell. Stem. Cell. 15, 707–719 (2014). [PubMed: 25456834]
6. Cui Q et al. m^6A RNA methylation regulates the self-renewal and tumorigenesis of glioblastoma stem cells. Cell Rep. 18, 2622–2634 (2017). [PubMed: 28297667]
7. Alarcón CR, Lee H, Goodarzi H, Halberg N & Tavazoie SF N^6-methyladenosine marks primary microRNAs for processing. Nature 519, 482–485 (2015). [PubMed: 25799998]
8. Liu N et al. N6–methyladenosine-dependent RNA structural switches regulate RNA-protein interactions. Nature 518, 560–564 (2015). [PubMed: 25719671]
9. Xiang Y et al. RNA m^6A methylation regulates the ultraviolet-induced DNA damage response. Nature 543, 573–576 (2017). [PubMed: 28297716]
10. Zhou J et al. Dynamic m^6A mRNA methylation directs translational control of heat shock response. Nature 526, 591–594 (2015). [PubMed: 26458103]
11. Liu J et al. m^6A mRNA methylation regulates AKT activity to promote the proliferation and tumorigenicity of endometrial cancer. Nat. Cell Biol. 20, 1074–1083 (2018). [PubMed: 30154548]
12. Huang H et al. Recognition of RNA N^6-methyladenosine by IGF2BP proteins enhances mRNA stability and translation. Nat. Cell Biol. 20, 285–295 (2018). [PubMed: 29476152]
13. Piekna-Przybylska D, Decatur WA & Fournier MJ The 3D rRNA modification maps database: with interactive tools for ribosome analysis. Nucleic Acids Res. 36, D178–D183 (2008). [PubMed: 17947322]
14. van Nues RW & Watkins NJ Unusual C'/D' motifs enable box C/D snoRNPs to modify multiple sites in the same rRNA target region. Nucleic Acids Res. 45, 2016–2028 (2017). [PubMed: 28204564]
15. Liu N et al. Probing N^6-methyladenosine RNA modification status at single nucleotide resolution in mRNA and long noncoding RNA. RNA 19, 1848–1856 (2013). [PubMed: 24141618]
16. Sergiev PV, Aleksashin NA, Chugunova AA, Polikanov YS & Dontsova OA Structural and evolutionary insights into ribosomal RNA methylation. Nat. Chem. Biol. 14, 226–235 (2018). [PubMed: 29443970]
17. Natchiar SK, Myasnikov AG, Kratzat H, Hazemann I & Klaholz BP Visualization of chemical modifications in the human 80 S ribosome structure. Nature 551, 472–477 (2017). [PubMed: 29143818]
18. Frye M, Harada BT, Behm M & He C RNA modifications modulate gene expression during development. Science 361, 1346–1349 (2018). [PubMed: 30262497]
19. Liu J et al. A METTL3-MEtTl14 complex mediates mammalian nuclear RNA N^6-adenosine methylation. Nat. Chem. Biol. 10, 93–95 (2014). [PubMed: 24316715]
20. Ping XL et al. Mammalian WTAP is a regulatory subunit of the RNA N^6-methyladenosine methyltransferase. Cell Res. 24, 177–189 (2014). [PubMed: 24407421]

Author Manuscript Author Manuscript Author Manuscript Author Manuscript

21. Wang X et al. Structural basis of N^6-adenosine methylation by the METTL3-METTL14 complex. Nature 534, 575–578 (2016). [PubMed: 27281194]
22. Bokar JA, Shambaugh ME, Polayes D, Matera AG & Rottman FM Purification and cDNA cloning of the AdoMet-binding subunit of the human mRNA (N6-adenosine)-methyltransferase. RNA 3, 1233–1247 (1997). [PubMed: 9409616]
23. Pendleton KE et al. The U6 snRNA m^6A methyltransferase METTL16 regulates SAM synthetase intron retention. Cell 169, 824–835.e814 (2017). [PubMed: 28525753]
24. Warda AS et al. Human METTL16 is a N6-methyladenosine (m6A) methyltransferase that targets pre-mRNAs and various non-coding RNAs. EMBO Rep 18, 2004–2014 (2017). [PubMed: 29051200]
25. Mendel M et al. Methylation of structured RNA by the m^6A writer METTL16 is essential for mouse embryonic development. Mol. Cell 71, 986–1000.e1011 (2018). [PubMed: 30197299]
26. Doxtader KA et al. Structural basis for regulation of METTL16, an S-adenosylmethionine homeostasis factor. Mol. Cell 71, 1001–1011.e1004 (2018). [PubMed: 30197297]
27. Albrecht M & Lengauer T Novel Sm-like proteins with long C-terminal tails and associated methyltransferases. FEBS Lett. 569, 18–26 (2004). [PubMed: 15225602]
28. Benhalevy D et al. The human CCHC-type zinc finger nucleic acid-binding protein binds G-rich elements in target mRNA coding sequences and promotes translation. Cell Rep. 18, 2979–2990 (2017). [PubMed: 28329689]
29. Jones MR et al. Zcchc11-dependent uridylation of microRNA directs cytokine expression. Nat. Cell Biol. 11, 1157–1163 (2009). [PubMed: 19701194]
30. Wen J et al. Zc3h13 regulates nuclear RNA m^6A methylation and mouse embryonic stem cell self-renewal. Mol. Cell 69, 1028–1038.e1026 (2018). [PubMed: 29547716]
31. Thomson E, Ferreira-Cerca S & Hurt E Eukaryotic ribosome biogenesis at a glance. J. Cell Sci. 126, 4815–4821 (2013). [PubMed: 24172536]
32. Wang X et al. N^6-methyladenosine-dependent regulation of messenger RNA stability. Nature 505, 117–120 (2014). [PubMed: 24284625]
33. Wang X et al. N^6-methyladenosine modulates messenger RNA translation efficiency. Cell 161, 1388–1399 (2015). [PubMed: 26046440]
34. Sloan KE et al. Tuning the ribosome: the influence of rRNA modification on eukaryotic ribosome biogenesis and function. RNA Biol. 14, 1138–1152 (2017). [PubMed: 27911188]
35. Arai T et al. Single methylation of 23 S rRNA triggers late steps of 50 S ribosomal subunit assembly. Proc. Natl Acad. Sci. USA 112, E4707–E4716 (2015). [PubMed: 26261349]
36. Khatter H, Myasnikov AG, Natchiar SK & Klaholz BP Structure of the human 80 S ribosome. Nature 520, 640–645 (2015). [PubMed: 25901680]
37. Punekar AS, Liljeruhm J, Shepherd TR, Forster AC & Selmer M Structural and functional insights into the molecular mechanism of rRNA m^6A methyltransferase Rlm. J. Nucleic Acids Res. 41, 9537–9548 (2013).
38. Golovina AY et al. The last rRNA methyltransferase of E. coli revealed: the yhiR gene encodes adenine-N6 methyltransferase specific for modification of A2030 of 23 S ribosomal RNA. RNA 18, 1725–1734 (2012). [PubMed: 22847818]
39. Wei J et al. Differential m^6A, m^6Am, and mlA. demethylation mediated by FTO in the cell nucleus and cytoplasm. Mol. Cell 71, 973–985.e975 (2018). [PubMed: 30197295]
40. Jia G et al. N6-methyladenosine in nuclear RNA is a major substrate of the obesity-associated FTO. Nat. Chem. Biol. 7, 885–887 (2011). [PubMed: 22002720]
41. Tang C et al. ALKBH5-dependent m^6A demethylation controls splicing and stability of long 3'-UTR mRNAs in male germ cells. Proc. Natl Acad. Sci. USA 115, E325–E333 (2018). [PubMed: 29279410]
42. Zhang S et al. m^6A demethylase ALKBH5 maintains tumorigenicity of glioblastoma stem-like cells by sustaining FOXM1 expression and cell proliferation program. Cancer Cell. 31, 591–606.e596 (2017). [PubMed: 28344040]
43. Li Z et al. FTO plays an oncogenic role in acute myeloid leukemia as a N^6-methyladenosine RNA demethylase. Cancer Cell 31, 127–141 (2017). [PubMed: 28017614]

Author Manuscript Author Manuscript Author Manuscript Author Manuscript

44. Liu F et al. ALKBH1-mediated tRNA demethylation regulates translation. Cell 167, 816–828.e816 (2016). [PubMed: 27745969]
45. Kawarada L et al. ALKBH1 is an RNA dioxygenase responsible for cytoplasmic and mitochondrial tRNA modifications. Nucleic Acids Res. 45, 7401–7415 (2017). [PubMed: 28472312]

References

46. Stojkovic V & Fujimori DG Radical SAM-mediated methylation of ribosomal RNA. Methods Enzymol. 560, 355–376 (2015). [PubMed: 26253978]
47. Ran FA et al. Genome engineering using the CRISPR-Cas9 system. Nat. Protoc. 8, 2281–2308 (2013). [PubMed: 24157548]
48. Hafner M et al. PAR-CliP-a method to identify transcriptome-wide the binding sites of RNA binding proteins. J. Vis. Exp. 41, 2034 (2010).
49. Esposito AM et al. Eukaryotic polyribosome profile analysis. J. Vis. Exp. 40, 1948 (2010).

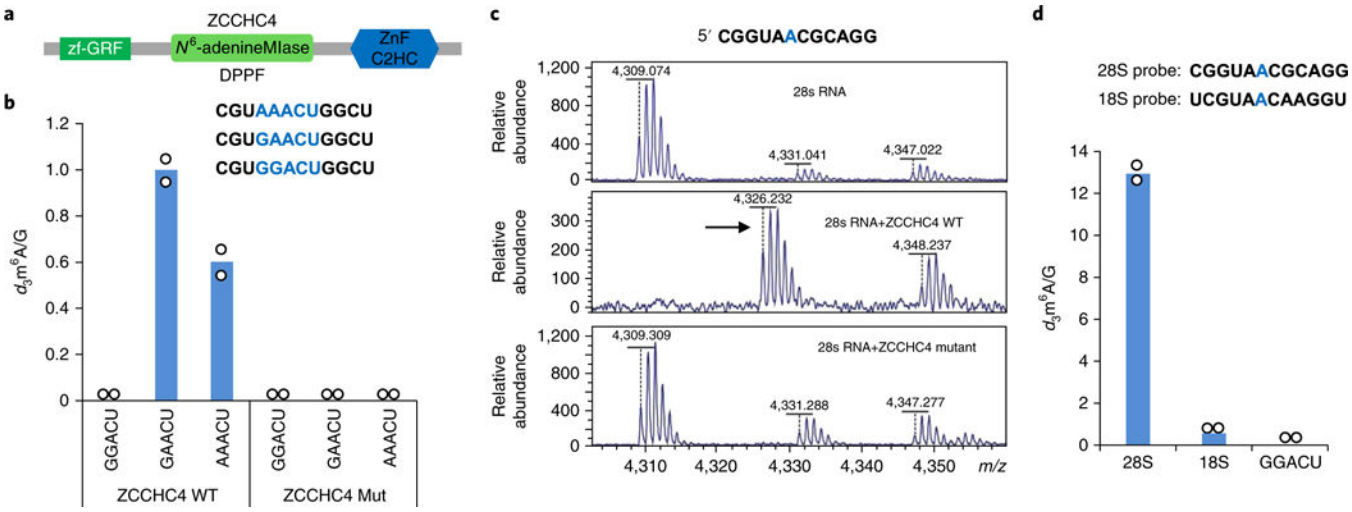

Fig. 1 |. ZCCHC4 methylates 28S rRNA in vitro.

a, Schematic representation of functional domains of human ZCCHC4. The DPPF motif corresponds to residues 276–279 of the protein. N^6-adeninMlase, N^6-adenine methyltransferase. **b**, Methylation activity of recombinant wild-type ZCCHC4 or catalytically dead mutant on RNA probes containing distinct sequence motifs (GGACU, GAACU and AAACU, indicated in blue). Enzyme activity was normalized to the GAACU oligo. $n = 2$, independent experiments. **c**, MALDI-MS analysis of 12-mer 28S rRNA oligos after reacting with d_3-SAM, wild-type or DPPF-AAAA-mutant ZCCHC4, respectively. A 17-Da peak shift appeared from 4,309 to 4,326 on 28S rRNA oligo after reaction with the wild-type enzyme. Black arrow indicates methylated peaks, and expected methylation site is shown in blue. This experiment was repeated independently three times with similar results. **d**, Methylation activity of recombinant ZCCHC4 on RNA oligos representing m^6A-containing 18 S and 28S rRNA; the expected m^6A site is shown in blue. GGACU oligo served as a negative control. $n = 2$, independent experiments.

Author Manuscript Author Manuscript Author Manuscript Author Manuscript

Author Manuscript Author Manuscript Author Manuscript Author Manuscript

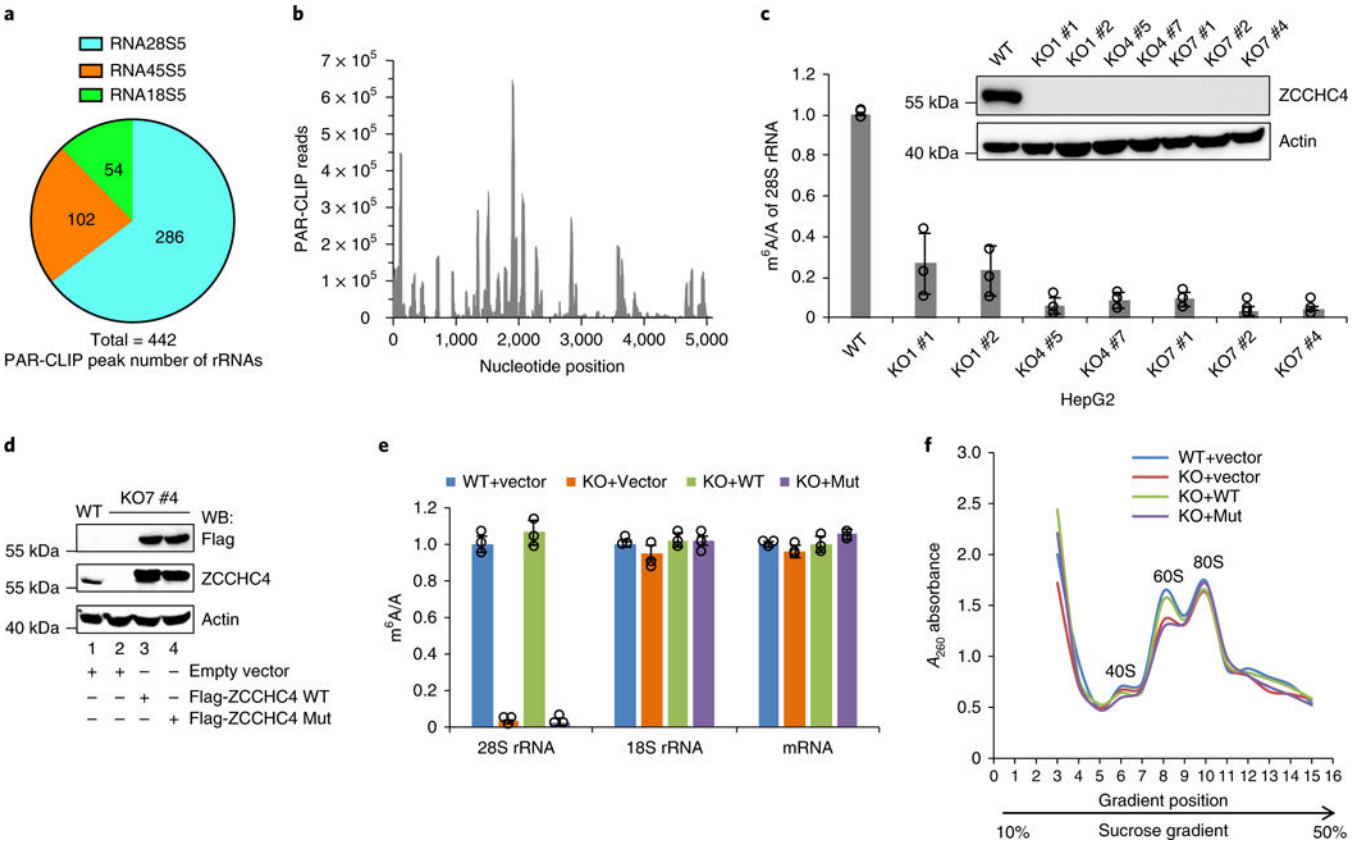

Fig. 2 |. ZCCHC4 catalyzes 28S rRNA methylation in cells.

a, PAR-CLIP peak number of ZCCHC4 on rRNA, showing that ZCCHC4 mainly binds 28S rRNA. This experiment was repeated twice with similar results. **b**, ZCCHC4 PAR-CLIP peaks of 28S rRNA. The highest covered region includes residues 1854–1913. **c**, LC-MS/MS showing m^6A/A level (relative to WT) of 28S rRNA in WT and KO cells, and western blotting analysis showing ZCCHC4 protein level in HepG2 cells. $n = 3$ independent experiments. Uncropped scans are shown in Supplementary Fig. 10. **d**, Cell lysates obtained from wild-type or *ZCCHC4* KO HepG2 cells rescued with indicated plasmids were subjected to western blotting analysis using flag, ZCCHC4, and actin antibody. This experiment was repeated twice with similar results. Uncropped scans are shown in Supplementary Fig. 10. **e**, LC-MS/MS showing m^6A/A levels (relative to WT) of 28S rRNA, 18S rRNA and mRNA from **d**. Error bars, mean ± s.d.; $n = 3$ biologically independent samples. **f**, Ribosomal subunit profiling by sucrose density gradient under low Mg^{2+} concentration (0.5 mM). This experiment was repeated twice with similar results. Wild-type HepG2 cells were transfected with empty vector and ZCCHC4 KO7 #4 cells were transfected with empty vector or wild-type flag-ZCCHC4 plasmid, or catalytically dead mutant flag-ZCCHC4 plasmid, respectively.

Author Manuscript Author Manuscript Author Manuscript Author Manuscript

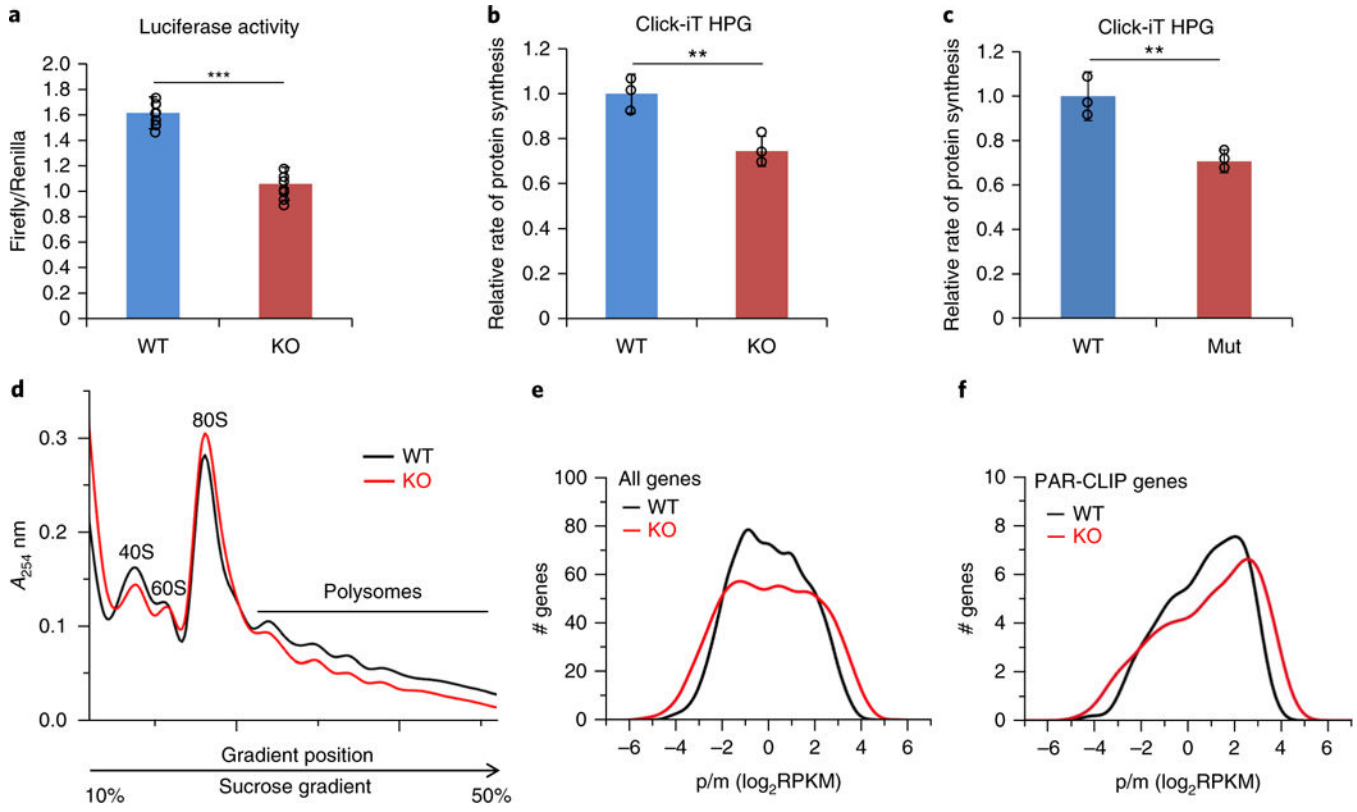

Fig. 3 |. ZCCHC4 activity affects translation.

a, *ZCCHC4* knockout affects translation of a luciferase reporter, indicated by Firefly/Renilla signal. Error bars, mean ± s.d.; $n = 8$ biologically independent samples. $^{***}P<0.001$. **b**, Click-iT L-homopropargylglycine (HPG) labeling showing that *ZCCHC4* knockout decreased global translation activity. Error bars, mean ± s.d.; $n = 3$ biologically independent samples. $^{**}P<0.01$. **c**, *ZCCHC4* KO cells were transfected with WT and catalytically dead mutant flag-ZCCHC4 plasmid. HPG labeling showing that ZCCHC4 mutant cells decreased global translation activity. Error bars, mean ± s.d.; $n = 3$ biologically independent samples; $^{**}P< 0.01$. **d**, *ZCCHC4* KO cells showing decreased polysome profiles in a sucrose gradient. This experiment was repeated twice with similar results. **e**, Histogram of polysome profiling sequencing results for all genes in *ZCCHC4* KO and WT cells. The *x* axis shows ratio of mRNA density in the polysome (*p*) divided by mRNA input (*m*); $n = 3$ biologically independent samples. **f**, Histogram of polysome profiling sequencing results comparing ZCCHC4 PAR-CLIP target genes in *ZCCHC4* KO and WT cells; $n = 3$ biologically independent samples.

Author Manuscript Author Manuscript Author Manuscript Author Manuscript

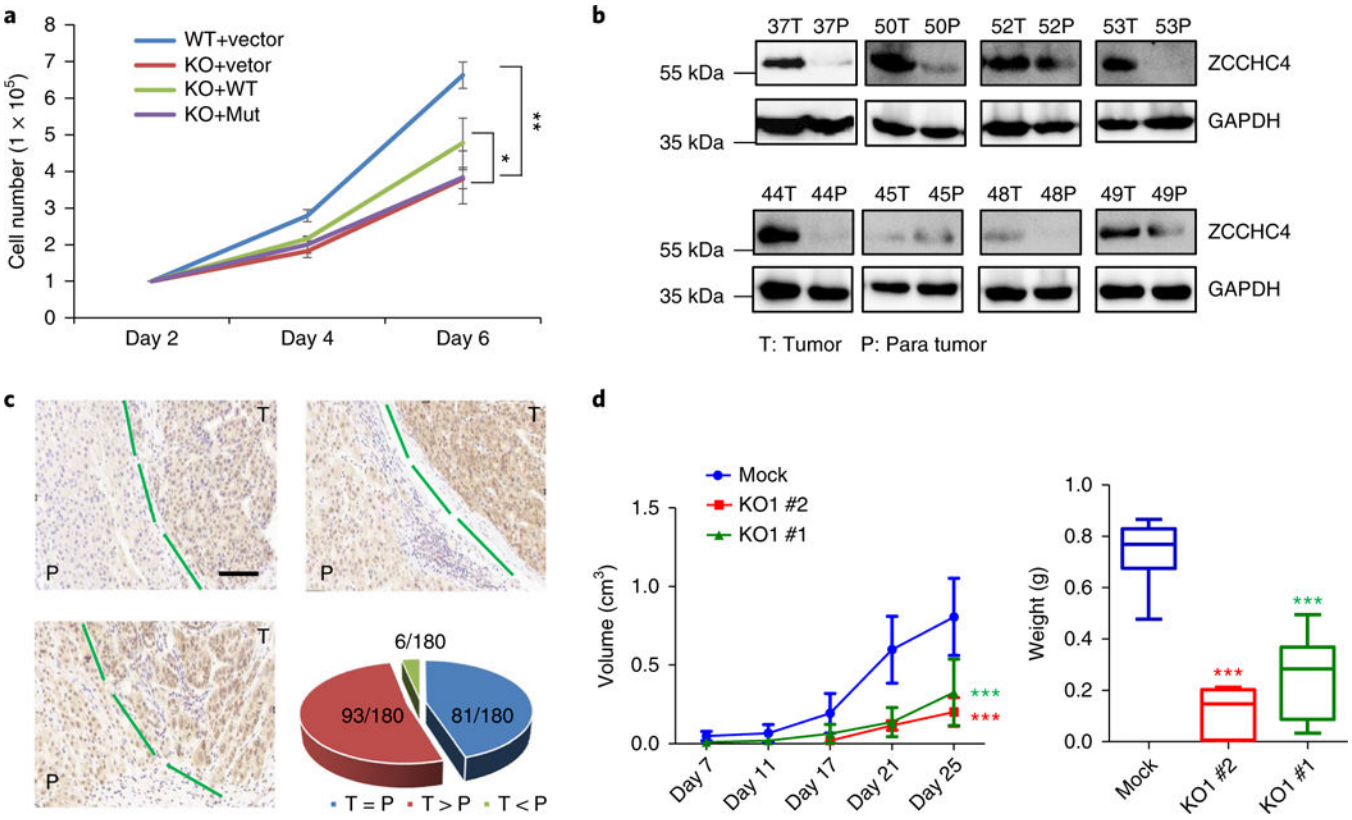

Fig. 4 |. ZCCHC4 expression in tumor tissues and its effects on xenograft tumor progression.

a, *ZCCHC4* knockout decreased proliferation of HepG2 cells, which could be rescued by wild-type ZCCHC4 but not by catalytic dead mutant. Error bars, mean ± s.d.; $n = 4$ biologically independent samples; $^{*}P<0.05$, $^{**}P< 0.01$. **b**, Protein lysates from liver cancer patient's tumor and para tumor tissues were subjected to western blotting using anti-ZCCHC4 and anti- GAPDH antibodies, respectively. This experiment was repeated twice with similar results. Uncropped scans are shown in Supplementary Fig. 10. **c**, IHC showing high expression of ZCCHC4 in a large portion of human liver tumor (T) and para (P) tumor tissues. The three images are representative results showing tumor tissues having higher expression of ZCCHC4 than para tissues, indicated by the DAB staining (in brown). Tumor tissues and para tissues are divided by dashed green lines. Pie chart shows number of tumors that show higher (red), same (blue) and lower (green) ZCCHC4 levels compared to para tissue; scale bar, 100 μm. **d**, HepG2 wild-type, KO1 # 1 and KO1 # 2 cells (~5×10^6) were used to establish subcutaneous (SC) xenograft tumor models. *ZCCHC4* knockout cells showed significant regression of tumor growth (volume or weight) in the nude mouse model compared to WT cells. $n = 7$ biologically independent animals. Left, values are expressed as mean and s.e.m.; two-way ANOVA was used for comparisons between groups. Right, values are expressed with box and whisker plot: center line represents the median of the data set, the bottom of the box represents the 75th percentile, and the top of the box represents the 25th percentile, whiskers from minimum to maximum. Student's f-test and one-way analysis of variance were used for comparisons between groups. $^{***}P<0.001$.